Journal of Applied Physics

Electron generation and multiplication at the initial stage of nanosecond breakdown in water

Cite as: J. Appl. Phys. **129**, 103302 (2021); https://doi.org/10.1063/5.0044415
Submitted: 15 January 2021 . Accepted: 22 February 2021 . Published Online: 09 March 2021

Xuewei Zhang, and Mikhail N. Shneider

AIP Publishing

Journal of Applied Physics ARTICLE scitation.org/journal/jap

Electron generation and multiplication at the initial stage of nanosecond breakdown in water

Cite as: J. Appl. Phys. **129**, 103302 (2021); doi: 10.1063/5.0044415
Submitted: 15 January 2021 · Accepted: 22 February 2021 ·
Published Online: 9 March 2021

Xuewei Zhang[1] and Mikhail N. Shneider[2,a)]

AFFILIATIONS

[1]Frank H. Dotterweich College of Engineering, Texas A&M University-Kingsville, Kingsville, Texas 78363, USA
[2]Department of Mechanical and Aerospace Engineering, Princeton University, Princeton, New Jersey 08540, USA

Note: This paper is part of the Special Topic on Plasma-Liquid Interactions.
[a)]**Author to whom correspondence should be addressed:** m.n.shneider@gmail.com

ABSTRACT

Electrical breakdown of liquid dielectrics under nanosecond pulsed high voltage has been investigated extensively in the last decade. Prior studies have focused on either experimental characterization of the breakdown process and discharge plasma or formulation/verification of the electrostrictive cavitation mechanism of the breakdown initiation. There remain knowledge gaps toward a clear physical picture of how the first plasma is generated in a region saturated by nanoscale cavities created by electrostrictive forces in inhomogeneous fields at the nanosecond timescale. Initial plasma results from the multiplication of primary electrons that gain energy collisionlessly in the cavities to cause collisional ionization of water molecules on the cavity walls. This paper quantitatively discusses the possible sources of primary electrons that seed the plasma discharge. Electron detachment from hydroxide is shown to be the most probable and sustainable electron source. Using numerical modeling, this study demonstrates the plausibility of an electron multiplication mechanism involving two neighboring cavities. The drift of hydrated electrons from one cavity to the next is the rate-limiting step and sets the minimum electric field requirement. This work will inform subsequent experimental studies and have implications in various applications such as plasma sources in biomedical applications, cavitation study, and insulation of pulsed power equipment.

I. INTRODUCTION

Electrical breakdown of liquid dielectrics under nanosecond (ns) or sub-nanosecond (sub-ns) pulsed high voltage has been investigated extensively in the last decade.[1–7] This is a relatively new research area that is of fundamental importance to plasma sources for biomedical applications[8,9] and insulation of pulsed power equipment.[10,11] For water in particular, the understanding of the mechanisms and processes of ns/sub-ns breakdown also sheds new light on cavitation research,[12,13] promising accurate determination of cavitation threshold pressure, which has many practical implications, such as informing fluid machinery design to reduce cavitation damage and generating cavities for targeted drug delivery.

Previous studies have focused on either experimental characterization of the breakdown process and discharge plasma[1,2] or formulation and verification of the electrostrictive cavitation mechanism of the breakdown initiation.[3–6] The electrostrictive cavitation mechanism was proposed to account for (i) the ns breakdown field in water is about one order of magnitude lower than the expected value ($\sim 3 \times 10^9$ V/m) from the linear dependence on the ratio of field and density, (ii) Joule heating is insufficient to cause the formation of vapor bubbles at the electrode at the ns timescale (therefore the bubble mechanism does not apply), and (iii) the existence of "dark phase" and reignition at the falling edge of the pulse.[14] The qualitative picture of the electrostrictive cavitation breakdown process is summarized as follows.[7] In a needle-plane geometry, the strong inhomogeneous field can create a negative pressure (electrostriction) in the order of −10 MPa, and its relaxation (via flow compensation) requires a time >10 ns. This sets the stage for the nucleation and growth of cavitation nanocavities in water in the vicinity of the needle electrode. Inside cavities, electrons are accelerated by the field to energies exceeding the water molecule ionization potential (12.6 eV) and, when hitting cavity walls, generate more electrons, which eventually lead to breakdown.

In recent years, there have been some new developments in the theoretical understanding of the electrostrictive cavitation

mechanism. Considering a single cavity at the tip of the electrode, a study[15] numerically solved the radial expansion of the cavity. The initial cavity radius was set as several micrometers, and the time for significant growth was after 10 ns, both too large for the initial stage of ns breakdown in water. Nevertheless, an interesting conclusion was that the existence of nanocavities does not lead to liquid breakdown through the gas phase following the Meek–Loeb criteria. Two independent studies[16,17] developed improved multiphysics modeling frameworks to simulate cavitation and subsequent processes. Both used a gas discharge type model to simulate initial plasma formation via ionization in the liquid phase[16] or electron avalanche in the cavities.[17] Along the same line as the latter, a new work[18] using Geant4-DNA simulation toolkit attempted to model the secondary electron generation by a sequence of collisions with the wall of the cavity (assumed as a long tube, which seems unrealistic). In addition to the inconsistencies in mechanism(s) of electron multiplication that results in initial plasma presented in the above works, another fundamental question remains unanswered: what might be the source(s) of primary electrons that trigger the electron multiplication process?

This paper, built upon our preliminary reports at the 2019 and 2020 Gaseous Electronics Conference,[19,20] presents an analysis of possible origins of primary electrons, demonstrating that electron detachment from hydroxide (OH^- ion) is more probable than other known sources under the experimental conditions. Furthermore, a multi-cavity mechanism of the electron multiplication is proposed and shown to be in good agreement with both basic physics and experimental results. This work bridges current knowledge gaps toward a clear physical picture of how initial plasma is generated in a region saturated by nanoscale cavities at the ns timescale.

II. POSSIBLE SOURCES OF PRIMARY ELECTRONS

Before discussing the possible sources of primary electrons, it is necessary to set the stage, i.e., describing the cavitation zone at the initial stage of ns breakdown in water. According to the electrostrictive cavitation breakdown mechanism, under a strong, inhomogeneous, fast-switched electric field, ruptures of the liquid continuum can be caused by the negative electrostriction pressure,[7]

$$P_E = -0.5\alpha_E \varepsilon \varepsilon_0 E^2, \tag{1}$$

where the coefficient $\alpha_E = 1.5$ for water, ε is the relative permittivity (80 for water), $\varepsilon_0 = 8.85 \times 10^{-12}$ F/m is the permittivity of free space, and E is the intensity of the local electric field. When $E = 10^8 \sim 10^9$ V/m, the corresponding $|P_E| = 5.38 \sim 538$ MPa, which is much higher than initial hydrostatic pressure in the ns breakdown experimental settings (therefore, it is neglected in this work) and within a range similar to that of the experimentally determined values ($2 \sim 140$ MPa) of the cavitation threshold pressure (i.e., tensile strength) of water.[21] For simplicity, hereafter, we use symbol P to represent $|P_E|$.

Consider a spherical cavity in water with high negative pressures (its absolute value is much higher than the vapor saturation pressure; therefore, the cavity here can be assumed to be a vacuum). An analysis of force balance indicates that there exists a critical cavity radius, R_c, above which the cavity can sustain or expand. We have[13]

$$R_c = 2\sigma/P, \tag{2}$$

where $\sigma = \sigma_0/(1 + 2\delta/R_c)$, $\sigma_0 = 0.072$ N/m is the surface tension of water at room temperature, and δ is the Tolman parameter to account that the actual surface tension is lower when the cavity radius is comparable to the thickness of the water's transition layer. We assume that all cavities are spherical and have one uniform size. In the framework of Zel'dovich–Fisher nucleation theory, the rate of creation of cavities with critical radius R_c per unit volume is[13]

$$\Gamma_c = \frac{3}{4\pi R_c^3}\frac{k_B T}{2\pi\hbar}\exp\left(-\frac{4\pi\sigma R_c^2}{3k_B T}\right), \tag{3}$$

where Γ_c is the rate of generation of cavities, $k_B = 1.38 \times 10^{-23}$ J/K is the Boltzmann constant, T is the temperature (298 K in this work), and $\hbar = 1.05 \times 10^{-34}$ J · s is the Planck constant. As shown in Fig. 1, with R_c in the proximity of 1 nm, Γ_c is between an upper limit of the number density of water molecules ($\sim 10^{10}$ μm^{-3}) per ns and a lower limit of 1 per μm^3 per ns.

Now even with $E = 10^9$ V/m (2 to 3 times higher than the maximum electric field in actual experimental systems), if the cavities, once formed, do not expand, then the energy gain of an electron traversing the cavity is around 2 eV, much lower than the water molecule ionization potential ($I_w = 12.6$ eV). To enable electron multiplication, the initial cavities must undergo subsonic expansion at the sub-ns timescale (10–100 ps)[6] and reaches an "equilibrium radius" beyond which the resulting relief of negative pressure will no longer support cavitation inception and development. Due to the complexity of this process, it is unclear what exactly is the final radius R. We estimate

$$R \gtrsim \frac{1}{2}\frac{I_w}{eE_c}, \tag{4}$$

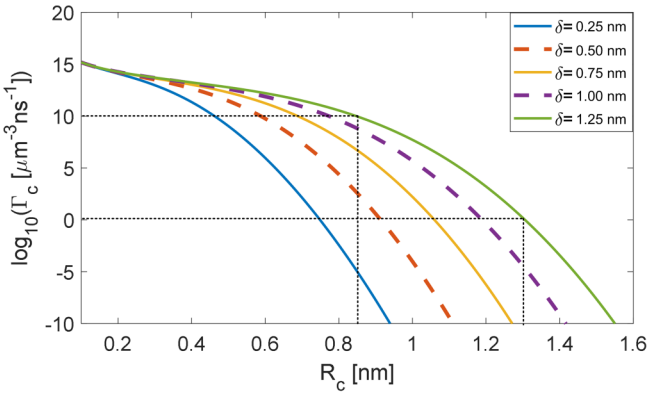

FIG. 1. Dependence of the rate of creation of cavities (Γ_c) on the critical cavity radius R_c and the Tolman parameter δ. The dashed lines mark the range of R_c (when $\delta = 1.25$ nm) that corresponds to physically reasonable Γ_c.

where $e = 1.60 \times 10^{-19}$ C is the electron charge and $E_c \approx 1.5E$ is the field intensity inside a nanocavity in the water where the local background field is E. The maximum number density of these cavities, n_c, can be estimated from that the pressure after relief by cavities remains comparable to P,[13]

$$n_c = \frac{fP}{Vc_s^2\rho}, \tag{5}$$

where $V = \frac{4\pi}{3}R^3$ is the cavity volume, f is a factor between 0 and 1, $\rho = 10^3$ kg/m^3 is the water density, and $c_s = 1.5 \times 10^3$ m/s is the speed of sound in water. In Fig. 2, we plot Eqs. (4) and (5) as a function of E. Stronger background fields result in smaller cavities and much higher cavity densities, consistent with the theoretical analysis in Eqs. (2) and (3).

In our simplified physical picture of the cavitation zone, at the sub-ns timescale, there are cavities that have the same radius and are uniformly distributed in the water. For instance, with $E = 0.42$ V/nm and $f = 0.9$, the corresponding $R = 10$ nm and $n_c \approx 1.2 \times 10^4$ μm^{-3}. The total volume of cavities takes up ~5% of the cavitation zone volume. If there are more than 20 electrons, then statistically speaking, one would be located within a cavity boundary to serve as the seed for breakdown. We proceed to examine the possible origins of primary electrons that satisfy the above condition.

The first possible source is cosmic background radiation. In the air, this creates $\sim 10^{-9}$ ions per μm^3. Although no data are found for water, it can be accepted that natural background radiation is highly unlikely to generate a greater degree of ionization in water.[7] Even assuming the density of cosmic radiation generated ions is proportional to the density of the medium, one can estimate that cosmic radiation might account for up to 10^{-6} ions per μm^3 in water (with or without cavitation), which, as will be shown below, is still a much less probable source compared to water's autoionization. The second possible source is field ionization of water molecules, which is negligible for fields lower than 7.5 V/nm.[7] The maximum field in experimental settings is an order lower than this

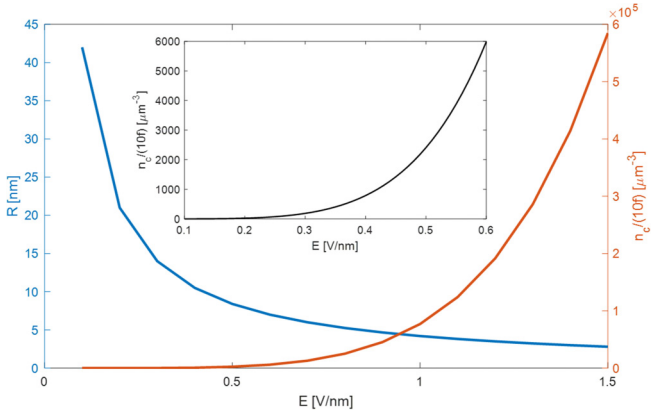

FIG. 2. The final cavity radius (R) and number density (n_c) as functions of the local background field. The inset shows n_c under low E.

value. Interestingly, even without radiation or strong field, water has autoionization ($H_2O + H_2O \rightleftharpoons OH^- + H_3O^+$):[22] at atmospheric pressure and 25 °C, the equilibrium density of hydroxide (OH^-) and hydronium (H_3O^+) ion pairs is 10^{-1} mol/m^3 or 60 per μm^3. Detachment from OH^- is the third and so far the most probable source of primary electrons. The reasons are as follows: (i) The electron detachment threshold of OH^- on surface (in our case, the cavity wall) is $I_n = 1.8$ eV,[23] much lower than that of OH^- in bulk (surrounding water molecules having stabilizing effects), as well as the water molecule's ionization potential I_w; (ii) OH^- ions tend to concentrate near the cathode-side pole of a cavity due to drift under the electric field; (iii) Strong electric field, especially in the order of 1 V/nm, can significantly enhance water autoionization;[24] (iv) The emission of electrons from the cathode-side pole into the cavity effectively shifts the equilibrium of water autoionization in that region rightwards (i.e., producing OH^- ions), which makes this mechanism sustainable.

To quantitatively demonstrate the above points (i) and (ii), we first build the physical model of a simple system consisting of a single spherical cavity in water, as shown in Fig. 3(a). The governing equations in water are

$$\frac{\partial c_i}{\partial t} + \nabla \cdot J_i = k \prod_i c_i, \tag{6}$$

$$J_i = -D_i \nabla c_i + z_i \mu_i F c_i \varepsilon, \tag{7}$$

$$\varepsilon = -\nabla \varphi, \tag{8}$$

$$\varepsilon_0 \nabla \cdot (\varepsilon \nabla \varphi) = -F \sum_i z_i c_i, \tag{9}$$

where t is the time, c_i ($i = H_3O^+$ or OH^-) represents the concentration (unit: mol/m^3) of each ion, $k = 1.5 \times 10^8$ mol^{-1}m^{3}s^{-1} is the equilibrium reaction rate constant of the water autoionization,[22] J_i is the flux of each species consisting of diffusion and drift where the diffusion coefficients[22] are $D_{OH^-} = 5.27 \times 10^{-9}$ m^{2}s^{-1} and $D_{H_3O^+} = 9.31 \times 10^{-9}$ m^{2}s^{-1}, and according to the Nernst–Einstein relation, the mobility of both ions is $\mu_i = D_i z_i e/(k_B T)$, $z_i = \pm 1$ is the charge number of ions, $F = 96\,485$ C/mol is the Faraday constant, ε and φ are the electric field and potential. Inside the cavity, only electric field equations are solved (Laplace's equation). There is no ion flux across the cavity wall. At $t = 0$, the field is applied, and the initial c_i's are the equilibrium value (10^{-4} mol/m^3). The model is implemented and solved in COMSOL Multiphysics 5.4 using coupled Electrostatics and Transport of Dilute Species modules. The dimension of the simulation domain is 200 nm for cavity radius 10 nm to ensure that the physical fields at the domain boundary take the "unperturbed" values.

In Fig. 3(a), the electric field inside the cavity is about 1.5 times the background field. Due to the low charge density, the field distribution is very close to the charge-free analytical solution and does not change over time. On the other hand, Fig. 3(b) shows that the hydroxide concentration is increased near the cathode-side pole of the cavity, which reaches a steady-state within 1 ns. By reducing the cavity size or increasing the background field, the steady-state

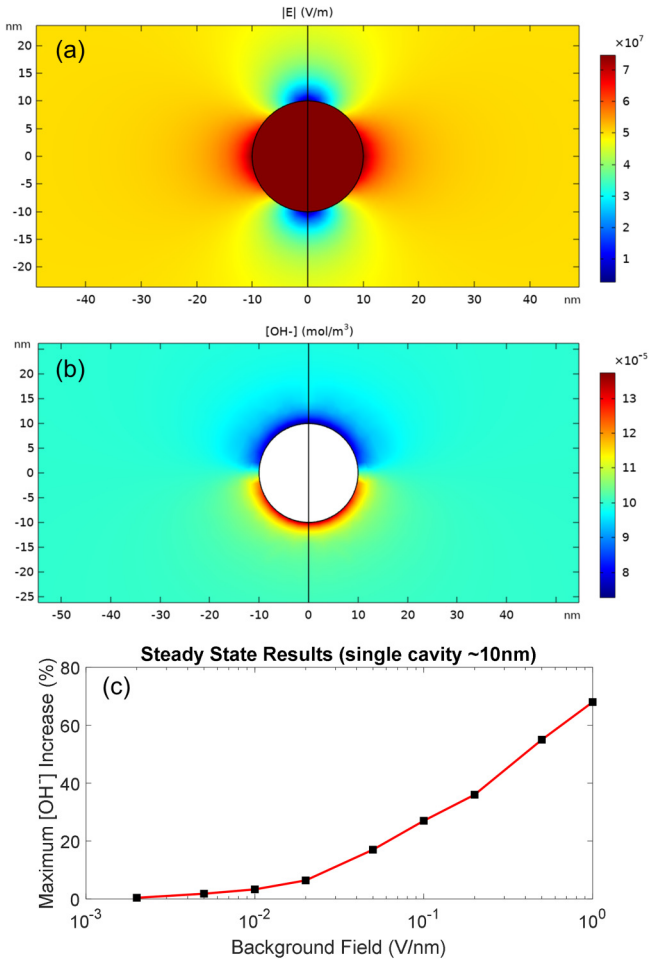

FIG. 3. Continuum multiphysics modeling results of a spherical cavity of radius 10 nm in water under electrostatic fields. (a) Distribution of the electric field magnitude when the background field is 0.01 V/nm. The arrow indicates the direction of the background field. (b) Steady-state hydroxide concentration under a background field of 0.2 V/nm. The steady-state is reached in less than 1 ns. (c) Increased hydroxide concentration at the cathode-side pole of the cavity (θ) as a function of the background field.

can be reached even faster, since the change of ion distribution results mainly from drift. Under different background fields, the maximum increased amount (denoted by θ) of OH^- concentration is plotted in Fig. 3(c). Note that the simulation domain is microscopic (the number of ions is small). The ion concentration at a location should be interpreted as the probability of finding an ion there.

The probability rate of tunneling detachment of an electron from an OH^- at the cavity wall can be estimated by[7]

$$w \approx \pi A^2 e E_c \sqrt{\frac{1}{2mI_n}} \exp\left(-\frac{4I_n^{3/2}\sqrt{2m}}{3\hbar e E_c}\right), \tag{10}$$

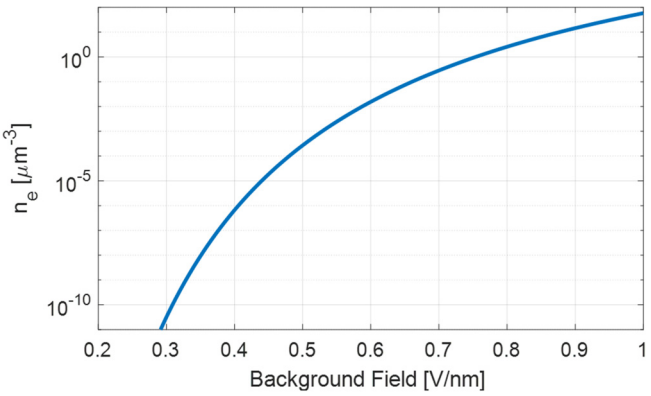

FIG. 4. Expected number density of electrons detached from hydroxide into the cavities within 0.1 ns as a function of the background field.

where $m = 9.11 \times 10^{-31}$ kg is the electron mass and the coefficient $A \approx 1$ depends on the potential well's shape. The number of electrons released into cavities per μm^3 during time $\Delta\tau$ is

$$n_e \approx w(1+\theta) n_{OH^-} \Delta\tau, \tag{11}$$

where $n_{OH^-} = 60\,\mu m^{-3}$ is the equilibrium hydroxide number density. In the context of ns breakdown, we expect the timescale of electron emission to be sub-ns. Here we choose $\Delta\tau = 0.1$ ns. Figure 4 plots Eq. (11) under various background fields. A background field higher than 0.75 V/nm correspond to an n_e above 1 per μm^3. For a cavity radius of 10 nm, the background field needs to exceed 0.42 V/nm for primary electrons to gain sufficient energy to trigger multiplication upon hitting the cavity wall. This field value corresponds to $n_e \approx 10^{-6}\,\mu m^{-3}$. If the volume of the cavitation zone is in the order of 0.1 mm^3, it would be very likely that one or more primary electrons are generated and released into the cavity. Using experimental techniques to determine the initial cavitation zone profile will be crucial to test the proposed theory.

III. ELECTRON MULTIPLICATION IN THE CAVITATION ZONE

The proposed electron multiplication mechanism is illustrated in Fig. 5. The basic idea is that multiple cavities are involved in this process. As mentioned earlier, within one nanoscale cavity, the primary electron is unlikely to gain sufficient energy to generate multiple new electrons under a background field of <1 V/nm. Other processes such as cavity deformation (stretch along the field line) and coalescence are not significant at the sub-ns timescale. The cavitation zone is saturated with nanoscale cavities that can be viewed as "frozen" in the discussion of the electron multiplication process. As shown in Fig. 5, the drift of hydrated electrons through the layer between two cavities (C) and the release of electrons when the hydrated electrons reach the second cavity (D) are the two steps that determine the effectiveness of the multiplication mechanism.

Denote the thickness of the inter-cavity layer as ΔL and the mobility of hydrated electron μ_h, and by requiring the time

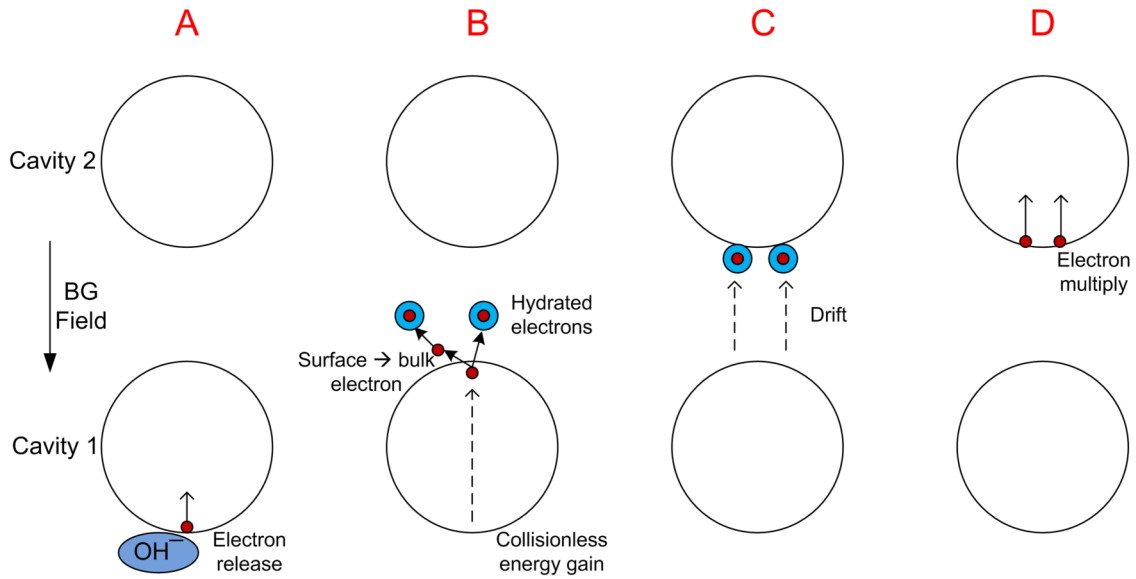

FIG. 5. Illustration of the proposed primary electron generation and multiplication mechanism. (a) Electron detachment from hydroxide ions and release into cavity 1. (b) After traverse cavity 1 collisionlessly, the electron gains sufficient energy to ionize a water molecule on the opposite wall of the cavity. The resulting two electrons enter the layer between cavity 1 and cavity 2 and immediately become surrounded by water molecules (hydrated electrons). (c) The hydrated electrons drift toward cavity 2. (d) The electrons freed enter cavity 2.

of travel across the layer to be at the sub-ns timescale (e.g., $\Delta\tau' = 0.2$ ns), we have

$$\frac{\Delta L}{\mu_h E_{av}} \lesssim \Delta\tau', \tag{12}$$

where E_{av} is the average magnitude of field in the layer, which can be obtained from the multiphysics modeling. Figure 6(a) presents a sample result when the layer separating the two cavities (both of radium 10 nm) is only 2 nm thick. In Fig. 6(c), we plot E_{av} (expressed as a percentage of the background field) as a function of ΔL in this case. While ΔL does not seem to have a significant effect on the hydroxide concentration at the cathode-side pole of cavity 1 [Fig. 6(b)], it affects E_{av} in the following way: when ΔL is smaller than the cavity radius, E_{av} is significantly lower than the background field; when ΔL becomes much larger than cavity size, each cavity can be treated as isolated and E_{av} is very close to the background field. The example in Fig. 6(a) also provides a clue regarding the difficulty of cavity coalescence. The substantial reduction of field reduces the amount of negative pressure and prevents the two cavities from being "pulled" closer.

The physical and chemical properties of hydrated electrons may vary greatly depending on the cluster size and the isomer type.[25] For the mobility of hydrated electron, we use 1.84×10^{-7} $m^2V^{-1}s^{-1}$ (close to that of OH^- in water).[26] To meet the condition in Eq. (12), the minimum background field is calculated and plotted in Fig. 7 as a function of ΔL. As expected, when ΔL is large, the field and, therefore, the drift velocity is proportional to ΔL. When ΔL is smaller than 10 nm, a higher background field is needed to counter the shielding effect. On the other hand, the cavity number density is related to ΔL,

$$n_c = \frac{1}{(\Delta L + 2R)^3}. \tag{13}$$

Combining Eqs. (13), (5), and (1), and set $R = 10$ nm in this case, we find another minimum background field. Figure 7 shows that, in this case, 3–12 nm is identified as the most "feasible" range of ΔL because as long as the field is high enough to create the cavities, the field is automatically able to make the electron drift ΔL within time $\Delta\tau'$. A theoretical implication is that there could be scenarios resulting only in cavitation but not electron multiplication.

Finally, we discuss the release of electrons into cavity 2. Using the formula similar to Eqs. (10) and (11),

$$w' \approx \pi A^2 e E_c \sqrt{\frac{1}{2mI_s}} \exp\left(-\frac{4I_s^{3/2}\sqrt{2m}}{3\hbar e E_c}\right), \tag{14}$$

$$N_e' \approx 2w'\Delta\tau, \tag{15}$$

where w' is the probability rate of the detachment of hydrated electron, I_s is the electron's affinity energy, and N_e' is the expected number of electrons entering cavity 2 (from the two hydrated electrons). In the literature, I_s values are found to be in a wide range from 0.1 to 0.3 eV (bulk) and 0.8 (surface)[27] to 1.3 eV[28] and to over 3 eV.[25] In Fig. 8, we pick three values in this range and plot N_e' as a function of the background field. With the electron affinity

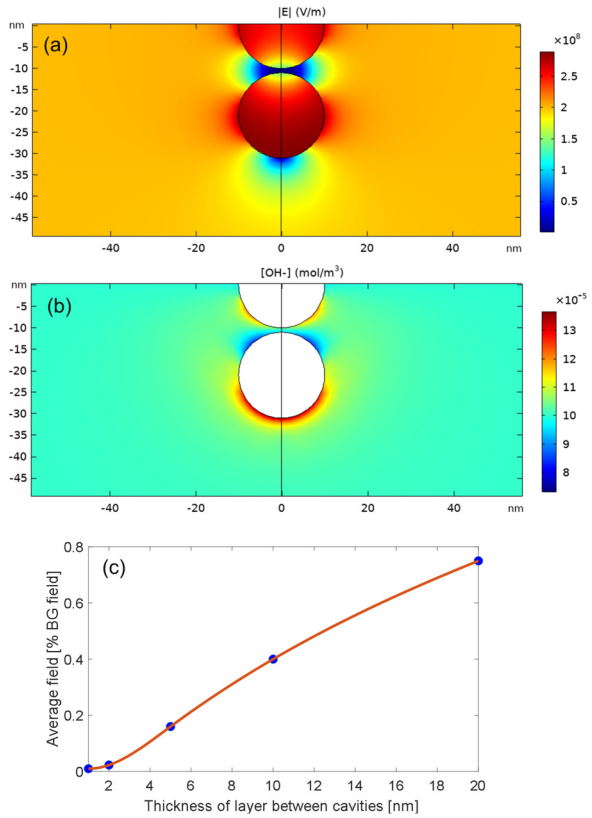

FIG. 6. Continuum multiphysics modeling results of two spherical cavities of radius 10 nm in water under a background field of 0.2 V/nm. (a) Distribution of electric field magnitude. (b) Steady-state hydroxide concentration. (c) Average field intensity in the liquid layer between the two cavities (expressed as a percentage of the background field) as a function of the layer's thickness.

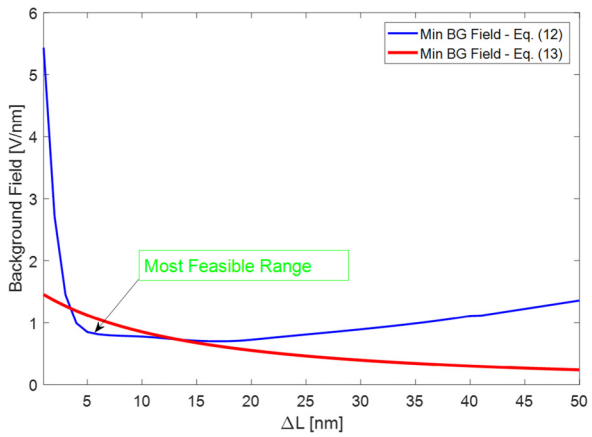

FIG. 7. The minimum background field required to enable the electron drift through the inter-cavity layer within $\Delta\tau'$ and the minimum background field needed to achieve the cavity number density as functions of the layer's thickness.

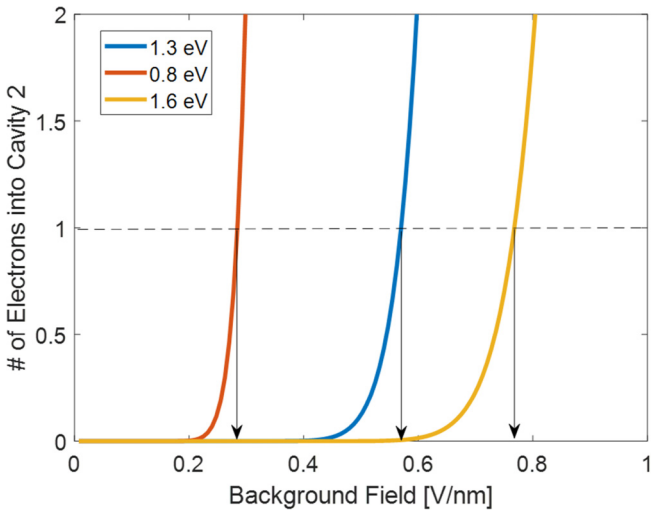

FIG. 8. The expected number of electrons entering cavity 2 via tunneling detachment as functions of the background field under three values of the electron's affinity energy.

energy in the range of 0.8–1.6 eV, the background field in the experimentally realized order of magnitude can ensure that >1 electrons are released into cavity 2. Electron multiplication will then follow this "chain reaction" path.

IV. CONCLUSIONS

This paper proposes a theoretical model of the generation and multiplication of primary electrons at the early stage of electrical breakdown in water under nanosecond pulsed fields, based on a simplified physical picture of the cavitation zone caused by electrostriction (negative electrical pressure). Several possible sources of primary electrons are identified. Even without the electric field, abundant hydroxides (OH^-) exist in water due to its autoionization. Electrons in hydroxide have a much lower detachment energy than water's ionization energy. It has been shown that electron detachment from hydroxide has the potential to be a major electron source. In addition, preliminary numerical results indicate that, at the ns timescale, the proposed multiplication mechanism involving hydrated electrons drifting toward the next cavity works. The required electric field strength and inter-cavity distance are physically plausible.

Subsequent work may be done in three directions. First, breakthroughs in experimental measurements of the cavitation inception and development will inform the revision and improvement of the theoretical methods used to analyze cavity size and density. Second, based on the proposed mechanism, new kinetic models coupled with multiphase electrohydrodynamics and advanced numerical simulation techniques could lead to a clearer understanding of the complex processes involved. Finally, this research opens up possibilities to use ns breakdown in water as a vehicle to investigate challenging problems in other fields, such as the pressure threshold for cavitation and the physical properties of hydrated electrons.

ACKNOWLEDGMENTS

This work is partially supported by the Princeton Collaborative Research Facility (PCRF), supported by the U.S. Department of Energy (DOE) under Contract No. DE-AC02-09CH11466. X.Z. also receives support from the U.S. DOE Office of Science Award No. DE-SC0021182.

DATA AVAILABILITY

The data that support the findings of this study are available from the authors upon reasonable request.

REFERENCES

[1]A. Starikovskiy, Y. Yang, Y. I. Cho, and A. Fridman, "Non-equilibrium plasma in liquid water: Dynamics of generation and quenching," Plasma Sources Sci. Technol. **20**, 024003 (2011).
[2]A. Starikovskiy, "Pulsed nanosecond discharge development in liquids with various dielectric permittivity constants," Plasma Sources Sci. Technol. **22**, 012001 (2013).
[3]M. N. Shneider, M. Pekker, and A. Fridman, "Theoretical study of the initial stage of sub-nanosecond pulsed breakdown in liquid dielectrics," IEEE Trans. Dielectr. Electr. Insul. **19**, 1579–1582 (2012).
[4]Y. Seepersad, M. Pekker, M. Shneider, A. Fridman, and D. Dobrynin, "Investigation of positive and negative modes of nanosecond pulsed discharge in water and electrostriction model of initiation," J. Phys. D: Appl. Phys. **46**, 355201 (2013).
[5]M. N. Shneider and M. Pekker, "Dielectric fluid in inhomogeneous pulsed electric field," Phys. Rev. E **87**, 043004 (2013).
[6]M. N. Shneider and M. Pekker, "Pre-breakdown processes in a dielectric fluid in inhomogeneous pulsed electric fields," J. Appl. Phys. **117**, 224902 (2015).
[7]M. N. Shneider and M. Pekker, *Liquid Dielectrics in an Inhomogeneous Pulsed Electric Field*, 2nd ed. (IOP Publishing, 2019).
[8]P. J. Bruggeman *et al.*, "Plasma-lliquid interactions: A review and roadmap," Plasma Sources Sci. Technol. **25**, 053002 (2016).
[9]P. Lukes, J.-L. Brisset, and B. R. Locke, "Biological effects of electrical discharge plasma in water and gas-liquid environments," in *Plasma Chemistry and Catalysis in Gases and Liquids*, edited by V. I. Parvulescu, M. Magureanu, and P. Lukes (Wiley, 2012).
[10]J. Lehr and P. Ron, *Foundations of Pulsed Power Technology* (IEEE Press, 2017).
[11]F. A. M. Rizk and G. N. Trinh, *High Voltage Engineering* (CRC Press, 2014).
[12]M. N. Shneider and M. Pekker, "Cavitation in dielectric fluid in inhomogeneous pulsed electric field," J. Appl. Phys. **114**, 214906 (2013).
[13]M. Pekker and M. N. Shneider, "Initial stage of cavitation in liquids and its observation by Rayleigh scattering," Fluid Dyn. Res. **49**, 035503 (2017).
[14]M. Pekker *et al.*, "Initiation stage of nanosecond breakdown in liquid," J. Phys. D: Appl. Phys. **47**, 025502 (2014).
[15]D. V. Tereshonok, "Cavitation in liquid dielectric under nanosecond high-voltage impulse," J. Phys. D: Appl. Phys. **50**, 015603 (2017).
[16]A. C. Aghdam and T. Farouk, "Multiphysics simulation of the initial stage of plasma discharge formation in liquids," Plasma Sources Sci. Technol. **29**, 025011 (2020).
[17]Y. Li *et al.*, "Towards an improved understanding of nanosecond-pulse discharge initiation in water: From cavitation to electron multiplication," Plasma Sources Sci. Technol. **29**, 075005 (2020).
[18]Z. Bonaventura, P. Bilek, J. Tungli, and M. Simek, "Fast pulsed electrical breakdown of water: Electron multiplication in liquid ruptures," in *Virtual Gaseous Electronics Conference*, *October 5–9*, (American Physical Society, 2020).
[19]X. Zhang and N. M. Shneider, "On the source of primary electrons at the initial stage of nanosecond breakdown in water," in *Gaseous Electronics Conference*, *October 28–November 1* (American Physical Society, College Station, TX, 2019).
[20]X. Zhang and M. N. Shneider, "Electron generation and multiplication at the initial stage of nanosecond breakdown in water," in *2020 Virtual Gaseous Electronics Conference*, *October 5–9* (American Physical Society, 2020).
[21]F. Caupin and E. Herbert, "Cavitation in water: A review," C. R. Phys. **7**, 1000–1017 (2006).
[22]P. Atkins and L. Jones, *Chemical Principles: The Quest for Insight*, 5th ed. (W. H. Freeman, 2010).
[23]C. Petersen, J. Thøgersen, S. K. Jensen, and S. R. Keiding, "Electron detachment and relaxation of OH^-(aq)," J. Phys. Chem. A **111**, 11410–11420 (2007).
[24]A. M. Saitta, F. Saija, and P. V. Giaquinta, "*Ab initio* molecular dynamics study of dissociation of water under an electric field," Phys. Rev. Lett. **108**, 207801 (2012).
[25]J. M. Herbert and M. P. Coons, "The hydrated electron," Annu. Rev. Phys. Chem. **68**, 447–472 (2017).
[26]K. H. Schmidt and W. L. Buck, "Mobility of the hydrated electron," Science **151**, 70–71 (1966).
[27]A. P. Gaiduk, T. A. Pham, M. Govoni, F. Paesani, and G. Galli, "Electron affinity of liquid water," Nat. Commun. **9**, 247 (2018).
[28]R. E. Ballard, "The electron affinity of water and the structure of the hydrated electron," Chem. Phys. Lett. **16**, 300–301 (1972).